region 1590 to 2310 Å at ~17 Å resolution.
13. D. T. Hall *et al.*, *Astrophys. J.* **426**, L51 (1994).
14. N. Thomas, *J. Geophys. Res.* **98**, 18737 (1993).
15. The radial profile of the electron temperature T_e in the Io torus is approximately constant from ~5.7R_J to 6.7R_J and rises sharply outside 6.7R_J. The electron excitation rate is proportional to $e^{-\Delta E/k_B T_e}$, where ΔE is the energy difference between upper and lower levels of the transition and k_B is Boltzmann's constant. The extreme-UV transitions are on a very steep part of this exponential function, so that small changes in T_e produce large changes in the excitation rate. By contrast, the visible and far-UV transitions are on much flatter portions of the exponential curve, where small changes in T_e have relatively little effect on the excitation rate.
16. A. J. Dessler and T. W. Hill, *Geophys. Res. Lett.* **21**, 1043 (1994).
17. I. de Pater *et al.*, *Bull. Am. Astron. Soc.* **26**, 4 (1994).
18. J. T. Clarke *et al.*, *Science* **267**, 1302 (1995).

Auroral Signature of Comet Shoemaker-Levy 9 in the Jovian Magnetosphere

R. Prangé, I. M. Engle, J. T. Clarke, M. Dunlop, G. E. Ballester, W. H. Ip, S. Maurice, J. Trauger

The electrodynamic interaction of the dust and gas comae of comet Shoemaker-Levy 9 with the jovian magnetosphere was unique and different from the atmospheric effects. Early theoretical predictions of auroral-type processes on the comet magnetic field line and advanced modeling of the time-varying morphology of these lines allowed dedicated observations with the Hubble Space Telescope Wide Field Planetary Camera 2 and resulted in the detection of a bright auroral spot. In that respect, this observation of the surface signature of an externally triggered auroral process can be considered as a "magnetospheric active experiment" on Jupiter.

Inside the jovian magnetosphere, the comae of comet Shoemaker-Levy 9 acted as ionized bodies that disturbed the electrodynamical equilibrium of the magnetosphere-ionosphere system. As a result, a variety of plasma processes, depending on the geometry of the field lines and the characteristics of the comae (including the dynamo effect resulting from the motion of charged dust through the ambient plasma), were expected to trigger energetic particle precipitation along field lines into the jovian ionosphere (*1*). The observable signature of such precipitations is auroral-type collisionally excited emissions in the far ultraviolet (FUV) at the magnetic footprints of the nuclei.

Several issues made the study of such interactions different from other observations of the comet's collision. First, in contrast with atmospheric effects, some auroral signatures started long before the impacts, and the magnetic footprints of the fragments remained on the dayside, even when the nuclei reached the nightside (*2*). Second, the nature of magnetospheric effects was controlled by the relative geometry of the comae and the local jovian magnetic field (Fig. 1). Therefore, the effects were subject to the 10-hour rotation period of Jupiter, and we had to consider the comet path not in a fixed planetocentric frame of reference but in the corotating tilted magnetic frame of Jupiter (*3*). Third, by chance, the comet path sampled a variety of magnetospheric regimes, going from the day to the night sides, from dusk to dawn, and because of the latitude of the trajectory, near the polar cap boundary, from closed to open magnetic field lines. As an additional consequence, there were periods during which plasma interactions could give rise to conjugate auroral signatures in both hemispheres.

Auroral Features

Among the observations of the Hubble Space Telescope (HST) FUV Imaging Program (*4*), some were scheduled with the assistance of the magnetic field models described below. An unusual emission was observed on 20 July 1994. Four images were taken with the Wide Field Planetary Camera 2 (WFPC2) between 14:10 and 14:47 UT, within 1 hour of the collision of fragment P2 (*5*). The first two exposures (400 s) were taken with filters F160WB and F130LP, which isolate the H_2 Lyman bands. The last two (300 s) were taken with the Wood's filter F160WB only, providing the H Lyman α, H_2 Werner, and Lyman band emission (*4*). The images did not reveal any

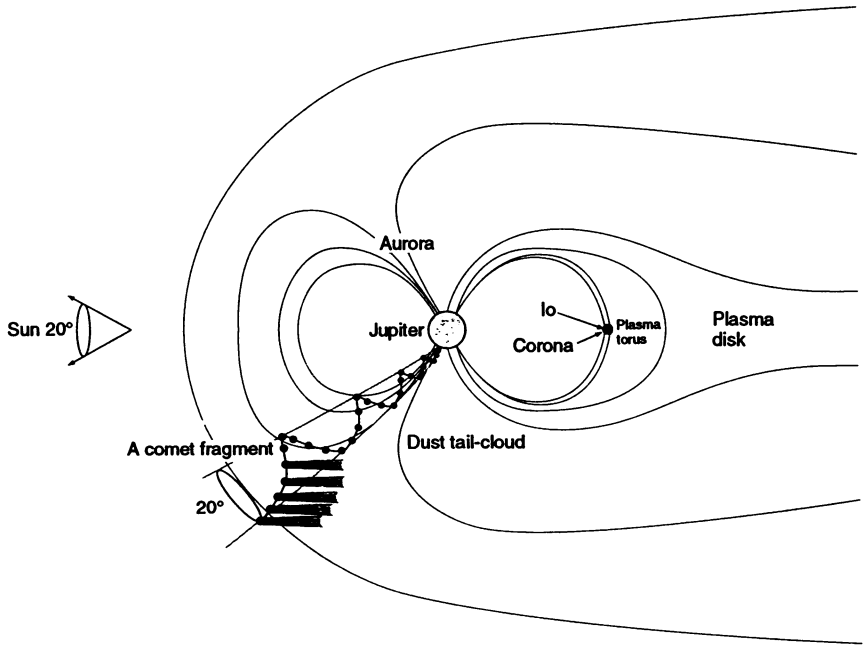

Fig. 1. Path of a fragment and its tail inside of the jovian magnetosphere (schematic) in the noon-midnight meridian. In the magnetic frame of reference, the trajectory is a pseudohelix, crossing alternatively open and closed field lines.

R. Prangé is with the Institut d'Astrophysique Spatiale, CNRS–Université Paris XI, 91405 Orsay, and the Institut d'Astrophysique de Paris, France. I. M. Engle is with the Physics Department, U.S. Naval Academy, Annapolis, MD 21402–5026, USA. J. T. Clarke and G. E. Ballester are with the Department of Atmospheric, Oceanic, and Space Sciences, University of Michigan, Ann Arbor, MI 48109–2143, USA. M. Dunlop is with the Space and Atmospheric Physics Group, Imperial College, London SW7 2BZ, UK. W. H. Ip is at the Max-Planck-Institut für Aeronomie, D-37191 Katlenburg-Lindau, Germany. S. Maurice is with the European Space Agency, ESTEC/SSD/SO, 2200 AG Noordwijk, Netherlands. J. Trauger is at the Jet Propulsion Laboratory, Pasadena, CA 91109, USA.

UV emission along the dawn limb. This does not contradict the theoretical prediction in that fragment P2 proved to make an impact much smaller than expected. By contrast, a feature was discovered on the polar cap: In all images, a similar auroral oval encircles the south pole (Fig. 2), but in one image (Fig. 2B), an additional bright spot appears, apparently inside the oval [there was a similar bright spot on the first image of the sequence (4, 6)]. We could not identify any magnetically conjugate spot in the north.

More than 2 years of observations with the HST's Faint Object Camera have given evidence that the morphology of the jovian aurorae is globally stable (although variable in intensity), with the brightest emissions localized along narrow ovals around the poles with, at times, a broad transpolar emission (7). The bright spot we discuss here is quite different from the classical morphology: It is on the polar cap, localized and modulated in brightness. For this reason, we have ruled out any "normal" mechanism (such as solar wind effects) that could already have produced similar features, and we have assumed that it was related to some interaction between the comet train and the magnetosphere, transmitted to the ionosphere by means of a field-aligned current system.

The high latitude of the emission and its apparent location in the early afternoon hemisphere rules out any effect from fragment P2. The later fragments, particularly the pair Q2-Q1, which immediately followed P2, are good candidates for the triggering of this unusual auroral spot. At the time of the observations, Q2-Q1 was about seven or eight jovian radii ($7R_J$ to $8R_J$) from the surface and 57° from the jovian noon meridian direction in the afternoon sector (8).

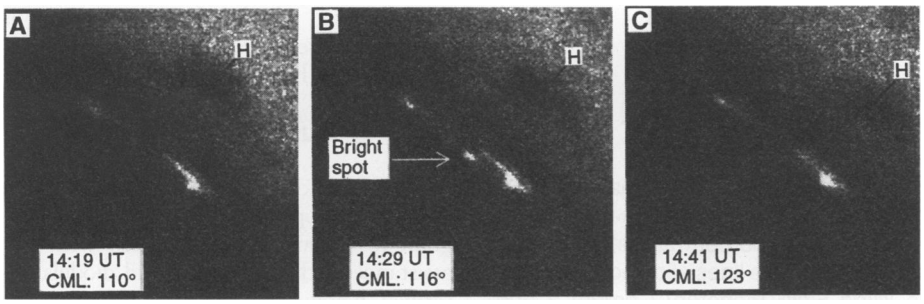

Fig. 2. Jupiter's south pole as seen in the last three FUV exposures from the HST WFPC2 on 20 July 1994, taken at (**A**) 14:19, (**B**) 14:29, and (**C**) 14:41 UT. Note the bright spot in (B). A similar spot was also observed at the same location on the first exposure of the series. The spot and the auroral oval are comparable in brightness (~250 and 500 kilorayleighs at maximum). The dark impact site of fragment H is seen rotating on the disk.

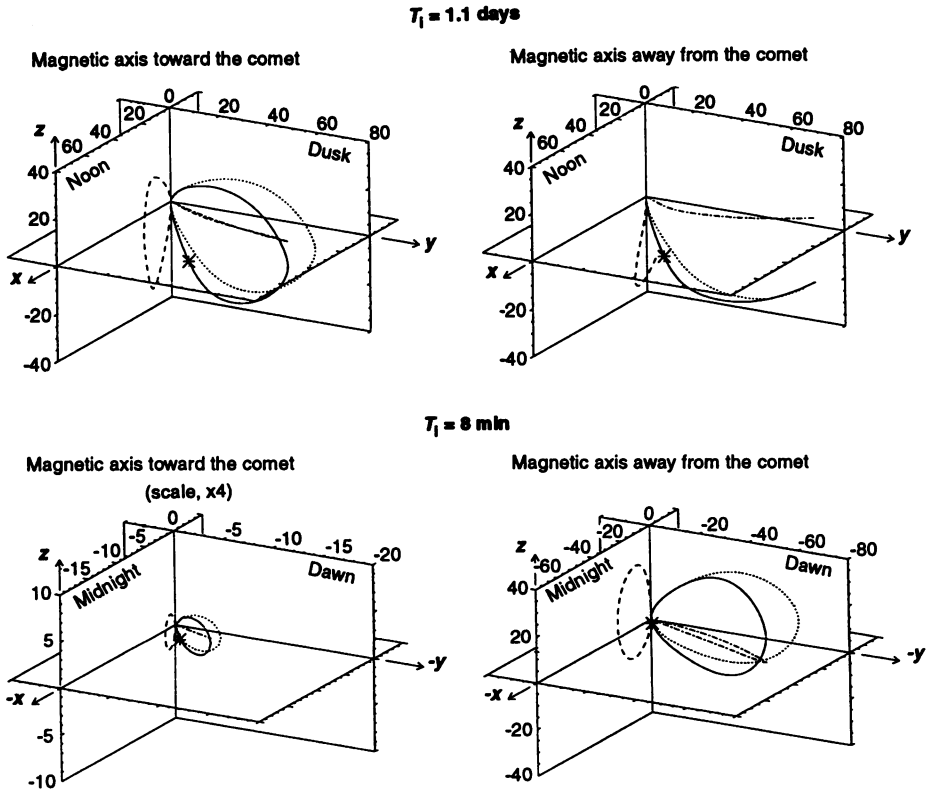

Fig. 3. Two typical examples of magnetic field lines as modeled taking into account the solar wind interaction and the direction of the jovian magnetic axis. For each date, two extreme configurations (north magnetic axis toward and away from the comet) lead to radically different field lines. A comprehensive set of such plots along the comet path was used to prepare the observations. The star indicates the location of the comet. Solid lines are field lines; dotted lines, dashed lines, and dotted-dashed lines are their *yz*, *xz*, and *xy* projections, respectively. T_i is the time until impact.

Modeling Jupiter's Magnetosphere

To study the relation between auroral emission and the fragment-charged environment, we had to map the instantaneous comet location down along magnetic field lines. We also had to characterize the nature of the field lines. Unfortunately, there does not yet exist any comprehensive model of the jovian magnetosphere that is valid from the magnetopause to the surface of the planet, and we had to combine the capabilities of two different models. The first is a version of the O_6 model (9), which allows the magnetic footprint of any inner- to middle-magnetosphere location to be calculated with a reasonably good accuracy, but which does not take into account the effects of the solar wind interaction at the outer boundary of the magnetosphere and is therefore unable to account for the shape of field lines far from the planet.

For the region far from the planet, we developed a three-dimensional model of the jovian magnetosphere that includes the 10-hour modulated variation of the magnetic axis. It superimposes the effects of the solar wind contribution to the magnetic field, as modeled by an internal source approximated by a planetary dipole, and an axially symmetric current sheet (therefore, it is not suited for near-surface simulations). It simultaneously calculates the shape of the magnetopause and the asymmetric deformation of the field associated with the current on this boundary driven by the solar wind (10) [we estimate that Shoemaker-Levy 9 crossed the magnetopause around $50R_J$ (11), which corresponds to a Voyager-type magnetosphere]. Any configuration of the jovian magnetic axis with the solar wind direction and the current sheet plane orientation can be represented, so that this model is able to follow the complex deformation of the instantaneous magnetic field lines passing

through any fragment of the comet as Jupiter rotates and as the comet travels across the magnetosphere (inwards, eastwards, and ultimately toward the nightside) (*10*). Figure 3 illustrates some of the major changes that can occur within a few hours, depending on the comet location: from dayside closed field lines to nightside open ones far from the planet (top) and from predawn closed field lines sweeping the inner to outer magnetosphere shortly before impact (bottom). It emphasizes how critically the nature of the field line depends on the comet's instantaneous parameters.

Field Line of Fragment Q

Using an impact decimal date of 20.83 July (*12*) (Q2 impacted 0.0056 day before this average date; Q1 impacted 0.0062 day after), we traced the surface magnetic footprints of the fragment as a function of time in both hemispheres with the first model. On the south polar projection (Fig. 4A), the footprint spirals toward the magnetic pole until 20.78 July (1.2 hours before impact) and then escapes toward lower latitude almost along a meridian to the impact site. The fraction of this track during which the bright spot was observed (20.57 to 20.62 July) is indicated on Fig. 2B as seen from Earth. For comparison, we also plotted the theoretical footprint of the magnetic shell $30R_J$ associated with the classical aurora. It appears that the magnetic footprint of fragments Q2 and Q1 was located on the planet and, with respect to the auroral oval, close to the bright spot observed at the same date, in terms of latitude as well as in terms of local time.

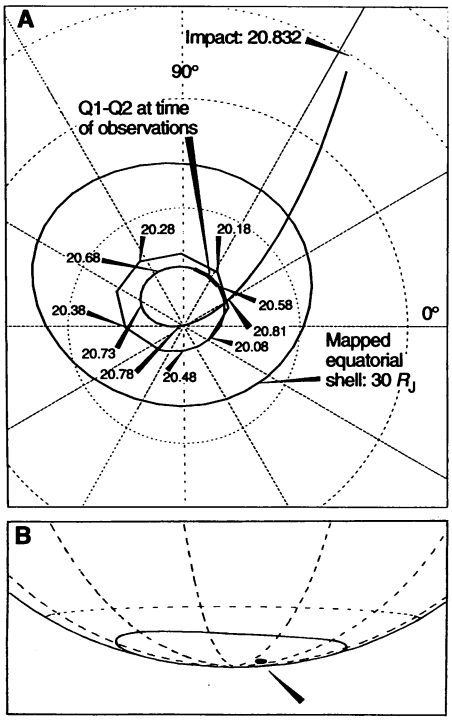

Fig. 4. (**A**) Polar projection of the comet's south magnetic footprint on the surface of Jupiter from 20 July 00:00 UT to impact time, created with a version of the O_6 model. The theoretical footprint of the $30R_J$ auroral oval is overplotted. (**B**) South footprints of Q1-Q2 and of the $30R_J$ oval during the observations, as seen from Earth.

At the northern conjugate footprint, the track vanished between 20.56 and 20.58 July (open field lines in the first model) and reappeared at 20.81 July: Our observations almost coincide with the transition from closed to open field lines (that is, the crossing of the polar cap boundary). However, because the first model does not properly describe high-latitude field lines, which are controlled by the relative geometry of the jovian magnetic axis and the solar wind direction, we used the second model to infer the nature of these field lines. Figure 5 shows the shape of the field line during the observations (~$7.5R_J$ from the surface, 140° between the comet and the magnetic north pole longitudes). The field line has its northern counterpart open in the tail. This is an important clue to interpret that no conjugate bright spot was observed in the northern hemisphere.

We have interpreted the transient bright spot as particle precipitation close to the footprint of fragments still in the magnetosphere, particularly of the pair Q2-Q1. Even if they did not give rise to the strongest impacts, these fragments were surrounded by the brightest and largest comae of the train (*13*): the motion of such an extended and dense ionized dust coma across the ambient magnetospheric plasma was favorable to the development of an intense current system flowing along magnetic field lines and closing through the fragment's conducting coma and the jovian ionosphere [as predicted by various investigators (*1*)]. If confirmed by further, more detailed studies, this event could be a unique example of a "magnetospheric active experiment" (*14*) in the jovian magnetosphere, in the sense used in studies of the Earth's magnetosphere for artificial injection of energetic particles or waves along magnetic field lines (from Earth's orbiting instrumentation) associated with the observation of ground signatures at the conjugate north and south surface footprints.

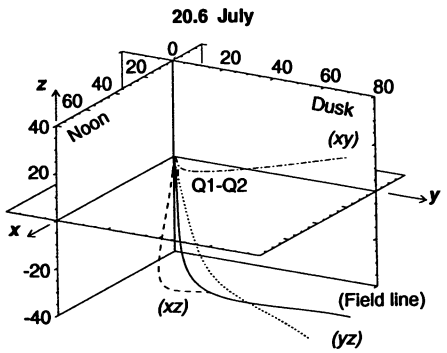

Fig. 5. Field line passing though fragments Q1-Q2 during the observations (20.6 July; 5.75 hours before impact).

REFERENCES AND NOTES

1. W. H. Ip and R. Prangé, *Geophys. Res. Lett.* **21**, 1051 (1994); W. Farrell *et al.*, *ibid.*, p. 1067; see also F. Herbert, *ibid.*, p. 1047; P. Kellog, *ibid.*, p. 1055; O. Bolin and N. Brenning, *ibid.*, p. 1063.
2. Auroral signatures occur more than 500 to 1000 km above the cloud tops for the ultraviolet emission and can be seen from the terrestrial vicinity above the planet limb.
3. In the corotating frame, the comet motion is a variable-radius, wobbling pseudohelix spiraling as a consequence of the periodic rotation of the jovian magnetic axis and the subsequent 10° wobbling of the magnetic equatorial plane.
4. The four images are presented by J. T. Clarke *et al.* [*Science* **267**, 1302 (1995)].
5. This date was selected, within HST's operational constraints, (i) on the basis of a theoretical prediction by W. H. Ip and R. Prangé for the most probable generation of current-driven precipitation along the last $2R_J$ of the fragment path (case of P2) and for extended comae (case of Q) and (ii) because magnetic field models predicted that conjugate south and north signatures were possible and observable from Earth.
6. The "blinking" nature of this spot is unexpected. It undoubtedly sets strong constraints on the nature of the physical mechanism triggering the particle precipitation in the fragment flux tube. We do not understand it at present, and in any event, the interpretation is out of the scope of this short report.
7. See, among others, J.-C. Gérard *et al*, *J. Geophys. Res.* **98**, 18793 (1993); J.-C. Gérard *et al*, *Planet. Space Sci.*, in press; and the review by R. Prangé, presented at Magnetospheres of the Outer Planets, Graz, Austria, 6 to 10 August 1994.
8. The ephemerides of the fragment trajectories in the magnetosphere were computed by P. Chodas (personal communication).
9. The O_6 magnetic field model [J. E. P. Connerney, M. H. Acuna, N. F. Ness, *J. Geophys. Res.* **86**, 8370 (1981); J. E. P. Connerney, in *Planetary Radio Emissions III* (Austrian Academy of Sciences, Vienna, 1992), vol. 13], derived from the Voyager magnetometer measurements, includes the contribution of multipolar terms of internal origin and of an equatorial current sheet between $5R_J$ and $60R_J$. We used a version of the O_6 model modified to account for Ulysses observations of Jupiter's magnetic field (M. K. Dougherty, personal communication).
10. See I. Engle, *J. Geophys. Res.* **96**, 7793 (1991) for the method as applied to Jupiter without the 10-hour modulation of the magnetic axis direction; I. Engle, *ibid.* **97**, 17169 (1992) for a tilted jovian magnetosphere; and I. Engle *et al.*, in preparation, for the full modeling of the instantaneous comet field lines.
11. This estimate is based on the detection of a transient emission line of Mg II at $53R_J$, associated with fragment G, by the Hubble Comet Science Team [P. D. Feldman, *Int. Astron. Union Circ. 6027* (18 July 1994)]. Enhanced ion emissions from the comae had been predicted as a consequence of the ionization of the coma material at the traversal of the jovian bow shock [A. S. Lipatov and A. S. Sharma, *Geophys. Res. Lett.* **21**, 1059 (1994)].
12. This value is based on the last predictions of impact times for fragments Q2 and Q1 of 19:47 and 20:04 UT, respectively, on 20 July (P. Chodas, D. Yeomans, Z. Sekanina, posted to the Shoemaker-Levy 9 electronic bulletin board, Planetary Data System

Small Bodies Node, University of Maryland). These ephemerides were accurate within ±10 min, but this does not affect our results because we study fragments far from the planet.
13. H. A. Weaver *et al*, *Science* **267**, 1282 (1995).
14. See, for instance, D. Mourenas *et al.*, *Planet. Space Sci.* **41**, 347 (1993).
15. We acknowledge funding by the Action Concertée Sol-Espace from the Centre Nationale d'Etudes Spatiales and Institut National des Sciences de l'Université, travel support from the European Space Agency to R. Prangé, and Space Telescope Science Institute grant GO-5624.18-93A to the University of Michigan. We thank P. Chodas for computing the ephemerides of the fragment trajectories in the magnetosphere for us. T. Bode significantly contributed to the development of the time-continuous magnetic field model.

The Fragment R Collision: W. M. Keck Telescope Observations of SL9

James R. Graham, Imke de Pater, J. Garrett Jernigan, Michael C. Liu, Michael E. Brown

The W. M. Keck telescope was used to observe the impact of comet Shoemaker-Levy 9 (SL9) fragment R at a wavelength of 2.3 micrometers on 21 July 1994. The data showed three outbursts. The first flash lasted about 40 seconds and was followed 1 minute after its peak by a second flash that lasted about 3 minutes. A third, longer lasting flare began 6 minutes after the first flash and lasted for 10 minutes. At its maximum brightness, the flare outshone Jupiter. The two short flashes are probably associated with the initial meteor trail and the subsequent fireball, respectively. The bright flare occurred when the impact site rotated into view. These data show that the explosion ejected material at least 1300 kilometers above the visible cloud tops. The luminosity of the impact site during the long bright flare was probably maintained by the release of gravitational potential energy, as this material fell back onto the lower atmosphere.

On 16 July 1994, the first fragment of comet Shoemaker-Levy 9 (SL9), fragment A, crashed into Jupiter, soon followed by fragments B through W. The observations presented here, which consist of a sequence of infrared images every 7.7 s, show the impact of fragment R and its immediate consequences. The observed response of Jupiter's atmosphere constrains the impact energetics and kinematics and provides a direct test of impact theory.

The 10-m W. M. Keck telescope (*1*) at Mauna Kea, Hawaii, was used to observe the impact of SL9 fragment R. The data were obtained with the facility near-infrared camera (*2*). The camera is equipped with a Santa Barbara Research Corporation InSb array (256 pixels by 256 pixels) and has a pixel size of 0.15 arc sec. We observed Jupiter with a narrow-band filter centered at a wavelength of 2.3 μm (wavelength, 2.28 to 2.31 μm). The planet is very dark at this wavelength, because sunlight is absorbed at 2.3 μm by CH_4 above Jupiter's cloud layers and only material at high altitudes, such as the high-altitude haze layers present above Jupiter's poles, stand out as bright features.

The authors are in the Department of Astronomy, Campbell Hall, University of California, Berkeley CA 94720, USA. J. G. Jernigan is also in the Space Sciences Laboratory, University of California, Berkeley.

Image Sequences: Moviemaking

We used the light-gathering power of the Keck telescope to obtain a record of the R event with many frames per minute. Data were taken in a movie mode, which yields one frame every 7.743 s, each with a total integration time of 4.347 s (*3*). The relative time of each frame is determined with reference to the quartz-controlled clock in the real-time system that controls the camera. The 1σ uncertainty in relative times is <10 ms. The real-time clock was synchronized to the observatory WWV and Global Positioning Satellite clocks. The systematic error in the absolute time is <0.5 s.

Three movie sequences were obtained, starting approximately 21 min before the expected fragment R impact [05:29 universal time (UT) (*4*)]. The first sequence runs from 05:08 to 05:18 UT, the second from 05:18 to 05:36 UT, and the third from 05:36 to 05:57 UT. There is a gap of a few seconds between each movie. Another sequence could not be obtained because the telescope was threatened by fog.

The movie shows two faint flashes on the limb at a latitude of ≈−44° (Fig. 1, panels 2 through 5) followed by a dramatic bright flare (Fig. 1, panels 7 and 8). The two flashes appeared as bright points on the limb in projection against the old G-D impact site complex. The end of the movie recorded the new R impact site rotating into view.

The first flash (Fig. 1, panel 2) was first seen at 05:34:44.5 UT (Table 1). In the next frame of the movie, the flash reached its peak, after which it decayed. The first flash was clearly visible only in five frames, or for 40 s. The rise time of the flash was ≈15 s, and the decline was slower, with an *e* folding time of ≈30 s. One minute later, a second flash occurred (Fig. 1, panel 4). This flash was also caught on the rise, but its decay was much slower with an *e* folding time of ≈180 s. Emission was visible for at least 180 s (Fig. 1, panels 5 and 6), when a third brightening occurred. There is some evidence for a brief brightening at the end of the second flash.

Almost immediately after the second flash faded, at about the expected time for the impact site to rotate into view (*4*), a new feature appeared on the limb (Fig. 1, panel 7). The new R impact site soon outshone the rest of the planet at this wavelength. The bright flare reached its maximum intensity (Fig. 1, panel 8) approximately 4 min after it became visible. Ten minutes after its first appearance, the intensity dropped to the level of that of the old G-D impact sites. As the bright flare faded and its emission returned to a level comparable to that of the G-D impact sites, a distinct change in the morphology of the emission region occurred (Fig. 1, panel 9). Up until this point the region was unresolved, but in the final 10 min of the movie the impact site was clearly resolved in a direction tangential to the limb with a length of ≈2 arc sec. Thus, in an interval of ≈1000 s, the impact had influenced a region of ≈7500 km. The lateral extent appeared to increase slightly until the final fading began. The D-G complex had moved off the limb by this stage, and the new impact site was clearly resolved from previous impact sites.

Figure 2A shows the 2.3-μm light curve of the R impact (*5*). The detector began to saturate when the brightness at 2.3 μm exceeded a magnitude of 3.3 [equivalent to 30 janskys (Jy), a unit of flux density, where 1 Jy = 10^{-23} erg s^{-1} cm^{-2} Hz^{-1}]. However, when the core of a stellar image is saturated there are still many unsaturated pixels in the wings of the point spread function. Photometry was recovered from saturated images by extrapolation of the flux measured in an unsaturated annular aperture with the use of the photometric curve of growth. We checked the reliability of this procedure by measuring the curve of growth before and after the fragment R event to ensure that it had not changed. Consequently, we can state with confidence that the flickering at the peak of the bright flare (Fig. 2A) is not an artifact.

The absolute scale of the photometry

Auroral signature of comet Shoemaker-Levy 9 in the jovian magnetosphere

R Prange, IM Engle, JT Clarke, M Dunlop, GE Ballester, WH Ip, S Maurice and J Trauger

Science **267** (5202), 1317-1320.
DOI: 10.1126/science.7871430